



The Current State and 125 Kyr History of Permafrost in the Kara Sea Shelf: Modeling Constraints

Anatoliy Gavrilov^{1,3}, Vladimir Pavlov⁴, Alexandr Fridenberg⁴, Mikhail Boldyrev⁵, Vanda Khilimonyuk^{1,3}, Elena Pizhankova^{1,3}, Sergey Buldovich^{1,3}, Natalia Kosevich^{1,3}, Ali Alyautdinov^{2,3}, Mariia Ogienko^{1,3}, Alexander Roslyakov^{1,3}, Maria Cherbunina^{1,3}, Evgeniy Ospennikov^{1,3}.

5

¹ Lomonosov Moscow State University, Geological faculty, Moscow, Russia

² Lomonosov Moscow State University, Geographic faculty, Moscow, Russia

³ Foundation «National Intellectual Resource», Moscow, Russia

⁴ Rosneft Oil Company, Moscow, Russia

10 ⁵ LLC «Arctic Research Center», Moscow, Russia



Abstract. The evolution of permafrost in the Kara shelf is reconstructed for the past 125 Kyr. The work includes zoning of the shelf according to geological history, compiling sea-level and ground temperature scenarios within the distinguished zones, and forward modeling to evaluate the thickness of permafrost and the extent of frozen, cold and unfrozen rocks. The modeling results are correlated to the available field data and are presented as geocryological maps. The formation of frozen, cold, and unfrozen rocks of the region is inferred to depend on the spread of ice sheets, sea level, and duration of shelf freezing and thawing periods.

1. Introduction

Permafrost studies and mapping in the Kara Sea shelf (Fig. 1) have a long history. The first evidence of its distribution in the Kara and other Eurasian Arctic shelves appeared in early permafrost maps of the USSR (Parkhomenko, 1937; Baranov, 1960). The extent and approximate thickness of the Kara shelf permafrost were first calculated numerically in the early 1970s (Chekhovsky, 1973). In the latest 1970s-earliest 1980s, Soloviev and Neizvestnov mapped the whole Russian shelf, and the work became part of the later 1:2 500 000 Geocryological Map of the USSR (1991). The dynamics of subsea permafrost in the Kara shelf during regression and transgression events was reconstructed by modeling (Danilov and Buldovich, 2001). Drilling was first used to study the features of permafrost and its recent formation in the near-shore zone of the Yamal Peninsula (Grigoriev, 1987).

Since 1986, drilling and seismoacoustic surveys have been run by the Arctic Marine Engineering Geological Survey (AMEGS) to constrain the extent of the Kara shelf permafrost and the depths to its top and base; the results were reported in a number of publications (Melnikov and Spesitvsev, 1995; Dlugach and Antonenko, 1996; Bondarev et al., 2001; Rokos et al., 2009; Kulikov and Rokos, 2017; Vasilyev and Recant, 2018). However, the available data are restricted to the southwestern part of the shelf while the more severe northeastern part remains poorly documented and undrilled.

Another recent map of permafrost distribution and thickness in the southwestern Kara shelf (Portnov et al., 2013) is based on seismoacoustic data and modeling with reference to the glacial eustatic curve but without regard to regional features related to the existence of MIS-3 marine terraces. Judging by drilling and seismoacoustic results from the western Yamal Peninsula shelf (Melnikov and Spesitvsev, 1995; Dlugach and Antonenko, 1996; Baulin 2001; Baulin et al., 2005; etc.), geocryological modeling has become quite realistic lately, but its quality is insufficient for economic activity, even within the best documented southwestern Kara shelf. As for the northeastern and central shelf parts, the knowledge is very preliminary.

The available permafrost maps refer to the datum sea depth of the maximum regression during the peak of cold stage 2 of the marine oxygen isotope stratigraphy (MIS-2). This reference is yet uncertain because the sea depths and level apparently varied in a range of at least tens of meters during the Late Pleistocene-Holocene glaciation history and related isostatic movements, as one may infer from the elevations of MIS-4 and MIS-3 marine terraces in Novaya Zemlya Islands which are raised high (Bolsiyanov et al., 2006). and the adjacent continent (Yamal, Gydan) terraces on which were formed at low sea level (-100 and -70 m respectively, Siddall et al., 2003; 2006)

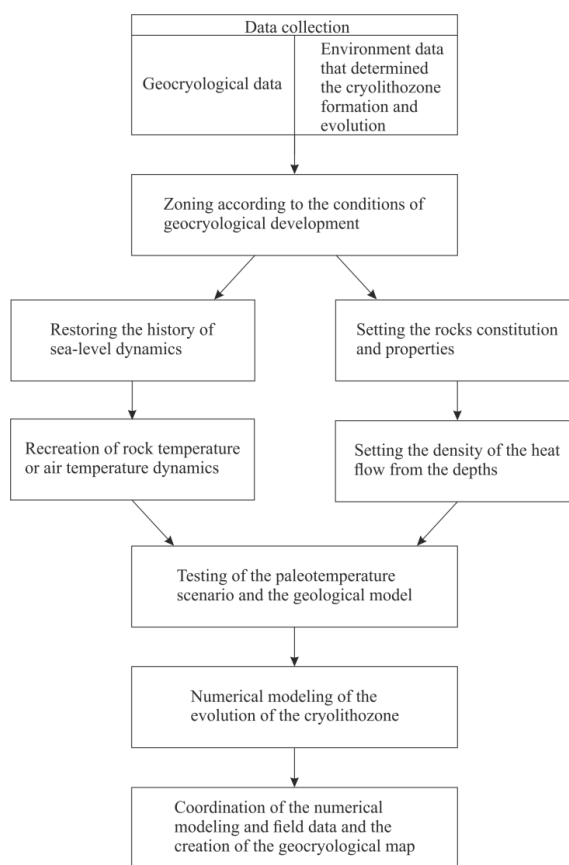
Given the logistic challenge and high costs of field studies, the knowledge of the Kara shelf permafrost can be extended by numerical modeling. Its application makes it possible to establish the connection of permafrost with components of the natural environment, including glaciations, glacio-isostatic movements, fluctuations in sea level, and so on.

2. Research methodology and its implementation

Permafrost in the Arctic shelf is mostly of relict origin: it formed during regressions and cold climate events and then degraded during Late Pleistocene-Holocene transgressions.



55 The methods for subsea permafrost research have been developed since the 1970s and use the retrospective
approach of reconstructing the permafrost evolution (Gavrilov, 2008; Romanovsky and Tumskoï, 2011). The history of
methods applied to study the structure and extent of permafrost of the eastern Russian Arctic was reviewed previously
(Gavrilov et al., 2001; Gavrilov, 2008; Nicolsky et al., 2012). We follow these methods in our work and are trying to
provide their progress. The work includes compiling a database of paleogeographic, geological, tectonic, and
geocryological results used further for dividing the region according to geological history and for creating possible
60 scenarios of sealevel and ground temperature variations. The general scheme of the methodology is presented in Figure 1.
The obtained estimates serve as boundary conditions in heat transfer modeling.



65 Fig. 1. The general scheme of the methodology.

The history of subsea permafrost has been modeled using software designed at the Department of Geocryology of the Geological Faculty in the Moscow State University (Khrustalev et al., 1994; Pesotsky, 2016). The software can solve Stefan's problems for non-steady state thermal conductivity assuming moving fronts of pore moisture phase transitions
70 within the modeling domain and variable boundary conditions. It provides a double-layer explicit solution obtained with the heat balance method, for an enthalpy problem formulation.

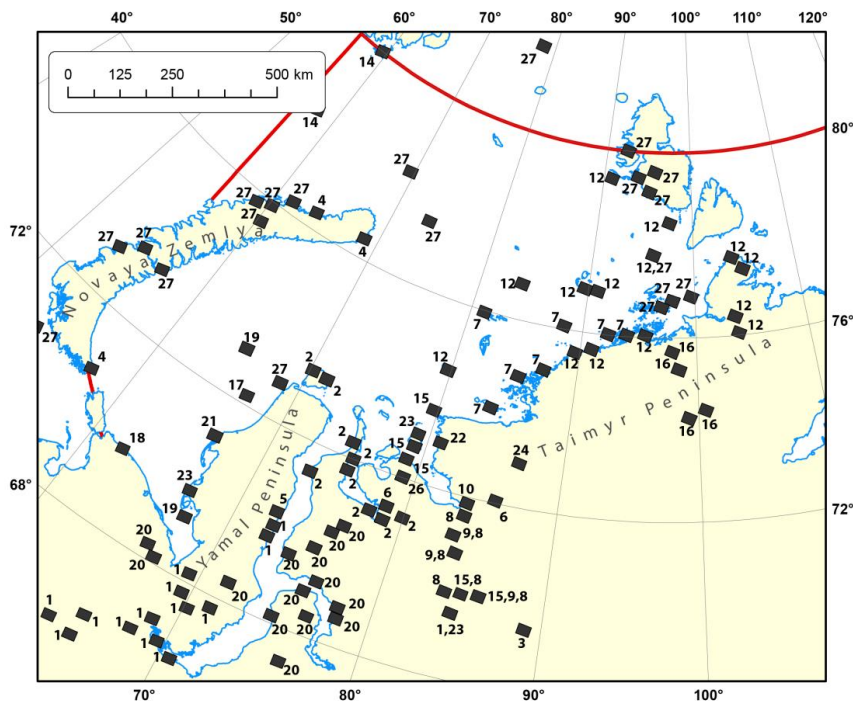


75 The permafrost dynamics was simulated for numerous paleoclimate scenarios that cover the full range of
presumable conditions in the Arctic shelves, including forty scenarios for the Kara shelf. The 1D modeling domain had a
vertical size of 5 km to avoid the effect of its base on the permafrost dynamics. The temperatures at the surface according
to the available paleoclimate reconstructions and a heat flux at the base of the modeling domain were used as the first- and
second order boundary conditions, respectively. The heat flux was assumed to be 50 mW/m², which corresponds to the
average for most of the shelf territory or 75 mW/m², as in zones of relatively high heat flux in gas-bearing bottom
sediments.

80 The modeling was performed for several uniform reference rock types in order to reduce the number of possible
solutions in the conditions of high lithological diversity in the area. Then the modeling results were extrapolated to
complex sections that comprise alternating reference lithologies or different combinations of relatively thick layers. All
rocks were assumed to be saline from top to bottom of the modeling domain. The paleotemperature scenarios and the
geological-tectonic model were tested by comparing the present permafrost state estimated by forward modeling with the
available field data from well documented areas, to achieve the best fit.

85 The evolution of the shelf permafrost was reconstructed by heat transfer modeling for the Late Pleistocene-
Holocene, since 125 kyr BP, the end of a long-term interglacial transgression. At that time, subsea permafrost had
presumably fully degraded over the whole studied part of the Kara Sea, and the temperatures of unfrozen bottom sediments
approached the steady state.

90 The modeling results were correlated with field data and both datasets were used for the final geocryological
division of the Kara shelf region. The Kara shelf has been quite well studied in terms of paleogeography. Figure 2 compiles
the various studies available for the paleogeography of this region.





95 Fig. 2. Late Pleistocene geology of the Kara region: data coverage. The numbers on the map correspond to the following publications:

Black squares are sites studied in different years by different research teams. Numbers 1 to 28 refer to publications:
1 = Astakhov and Nazarov (2010); 2 = Baranskaya and Romanenko et al. (2018); 3 = Bolshiyarov et al. (2007); 4 = Bolshiyarov et al. (2009); 5 = Vasil'chuk (1992); 6 = Geinz and Garutt (1964); 7 = Gusev et al. (2016a); 8 = Gusev et al. (2016b); 9 = Gusev et al. (2015a); 10 = Gusev et al. (2015b); 11 = Gusev et al. (2013a); 12 = Gusev et al. (2012a); 13 = Gusev and Molod'kov (2012); 14 = Gusev et al. (2012b); 15 = Gusev et al. (2011); 16 = Derevyagin et al. (1999); 17 = Kulikov and Rokos (2017); 18 = Leibman and Kizyakov (2007); 19 = Melnikov and Spesivtsev (1995); 20 = Nazarov (2011); 21 = Grigoriev (1987); 22 = Streletskaya et al. (2012); 23 = Streletskaya et al. (2015); 24 = Sulerzhitsky et al. (1995); 25 = Forman et al. (2002); 26 = Gilbert et al. (2007); 27 = Hughes et al. (2016); 28 = Svendsen et al. (2004).

105 3. Paleogeographic scenarios

The peculiarity of the paleogeography of the Kara region is the existence of a number of ideas about its development in the Late Pleistocene. Evaluation of the validity of these ideas and the selection of the most reasonable of them was one of the objectives of the present studies. The most popular are two controversial hypotheses implying the presence (Svendsen et al., 2004; Hughes et al., 2016) and absence (Gusev et al., 2012a) of ice sheets in the area. The absence of ice sheets is, however, inconsistent with the existence of (I) Late Pleistocene marine terraces in the Yamal and Gydan Peninsulas and (II) large unfrozen zones in the offshore extensions of major West Siberian rivers (Ob', Yenisei, Taz, and Gyda). The terraces most likely result from a 100 m sea level fall during the Zyryanian cold event (MIS-4). Their origin was possible only by subsidence and uplift due to ice loading (glaciation and low stand) and isostatic rebound (deglaciation and high stand), respectively. The unfrozen zone on the extension of the Ob', Yenisei, Taz, and Gyda rivers is detectable by drilling and seismic surveys run by AMEGS (Kulikov and Rokos, 2017). In our opinion, it formed in the place of a freshwater dammed lake (Fig. 3) that existed during the MIS-2 cold event when ice obstructed the continuing river flow. Currently, the largest part of the lake contoured according to the modern bathymetry looks like a shallow-water flat, which area occupies many hundreds of thousands of square kilometers. Within it, only the paleo-valley of the Ob is expressed, it is absent from the Yenisei. The insignificance of the severity of the ancient valley network is especially clearly seen when comparing it with that in the eastern sector of the Arctic, where there were no glaciations. Paleodoliny Khatangi-Anabar, Olenek, Lena, Indigirka, and Kolyma are clearly traced in bathymetry up to the outer shelf. The existence of a dammed lake produced by an ice dam during the MIS-2 cold event is recorded in the estuaries of the West Siberian rivers, which are much longer and farther advanced than those of any other river of the Eurasian Arctic basin. The duration of its existence is explained by the length of the Ob, Taz and Pur estuaries and their flatness. Both of these indicators are close to the record, if not the record for Eurasia: 800 km - the length of the Ob estuary and 1-2 cm / 1 km - the average longitudinal slope of its bottom.

Thus, the paleogeographic scenarios used by authors for reference in the modeling of this study assume the existence of ice sheets (Svendsen et al., 2004; Hughes et al., 2016). For the modeling purposes, the shelf is divided by authors into domains, subdomains, areas and subareas according to its 125 Kyr history of glaciations and the respective effects on bottom sediments (Fig. 3; Table 1).



Fig. 3. Division of the Kara shelf according to its geological history for 125 kyr. Abbreviations are explained in text and in Table 1.

135

The glacial domain includes zones where the MIS-2 ice sheet reached the sea bottom (G-1) and those of shelf ice at greater sea depths (G-2); the periglacial domain consists of subaerial and subaquial (under the ice-dammed lake) subdomains, which are further divided into areas of the present sea bottom (central shelf, C) and estuaries (E) within the subaquial subdomain and southwestern (SW) and northeastern (NE) shelf parts within the subaerial subdomain (Fig. 3; Table 1). The SW and NE areas had different landscapes during MIS-2 and, correspondingly, differed in ground temperature and frost depth. The areas C and E were flooded by cold ($<0^{\circ}\text{C}$) sea water and warmer ($>0^{\circ}\text{C}$) river water, respectively, in the Holocene.

140



Table 1. Zoning of the Kara shelf (Late Pleistocene-Holocene history, past 125 kyr, events MIS-2 – MIS-1)

145

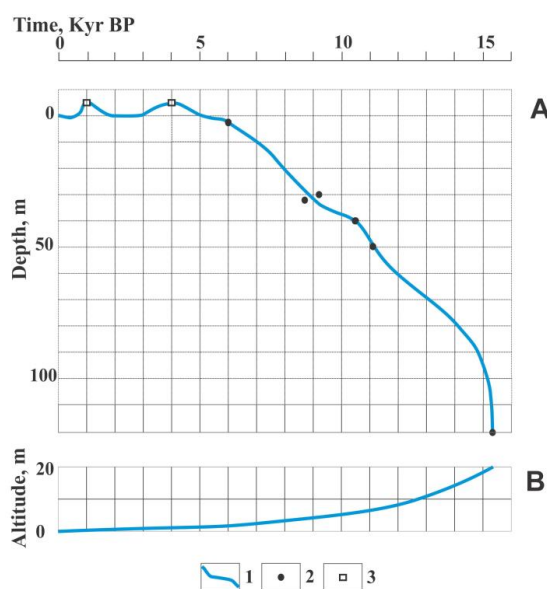
| Domains | Subdomains | Areas (landscapes) | | Subareas |
|--|-------------------------------------|--------------------|-----------|--|
| Periglacial domain | Subaerial | Southwestern shelf | SW | Sea depths 0-120 m (contour intervals of average depths at 5, 20, 50, 80 and 100 m) |
| | | Northeastern shelf | NE | |
| | Subaqual (under ice-dammed lake) | Central shelf | C | Sea depths 0-80 m |
| | | Estuaries | E | |
| Glacial domain, ice reaching sea bottom | Subaqual (for 7-10 Kyr) | G-1 | | Sea depths 0-200 m |
| Glacial domain, shelf ice, MIS-2 | Subglacial- subaqual | G-2 | | Sea depths 200-800 m |



150 Finally, the periglacial areas were divided into subareas according to sea depths which controlled the duration of permafrost formation during regressions and degradation during transgressions: 0-10, 10-35, 35-65, 65- 90 and 90-140 m sea depth intervals with average values of 5, 20, 50, 80, and 120 m, respectively.

155 The subdomains of ice reaching (G-1) or not (G-2) the sea bottom were revealed from seismoacoustic data, with reference to the 1:2 500 000 Map of Quaternary deposits (2010): transparent sequences (sea depths below 200 m) were interpreted as subglacial-subaqual (shelf) ice. The zones G-1 and G-2 are only shown in Fig. 3 and Table 1 and were not divided further. The modeling we carried out for the G-1 area showed that, to date, the MMPs formed in the MIS-2 have not survived.

160 The present permafrost in the region formed under the effect of climate-driven eustatic sealevel change. The sealevel curve for the 125-15 Kyr period was plotted using the eustatic curves of Lambeck and Chappell (2001) and Siddal et al. (2003, 2006). These curves were adapted to the regional specificity (Trofimov et al., 1975; Streletskaia et al., 2009; The State Geological Map, 2015), with regard to Late Pleistocene marine terraces in Yamal interpreted in the context of ice waxing and waning. Special focus by authors was in the recreating on the Late Pleistocene-Holocene transgression (Fig. 4).



165 Fig. 4. Late Pleistocene-Holocene transgression and shelf flooding (was drawn up by Gavrilov A.V.).
A: periglacial domain 1 = sealevel curve, from 15 Kyr BP to Present; 2 = dated bottom sediment cores from Ob' Gulf, Yenisei Gulf, and adjacent offshore (Stein, R. et al., 2009) and Vilkitsky Strait (Levitan, M.A. et al., 2007) sites; 3 = onshore data (Romanenko, F.A., 2012);
B: glacial domain.

170 In the method of constructing a scenario of sea level fluctuations for the Karsky shelf, the accounting for glacio-isostatic movements, resulting in the formation of marine terraces (Gutenberg, 1941; Flint, 1957; Bylinsky, 1996), plays a large role. The reason for their formation is the flooding of the sea by the end of the glacier lowered glacier bed, with a lag reacting to a rise of the removal of the glacial load. Therefore, during reconstructions, post-glacial sea level fluctuations are divided into two categories. In non-glacial areas, sea level rises in relation to the nearest coast, in glacial areas it drops
175 (Lambeck, Chappell, 2001).



In accordance with the above, the scenario is presented in the form of curves for the periglacial (with respect to the continent, Fig. 4A) and glacial (with respect to Novaya Zemlya, Fig. 4B) domains. The periglacial curve was obtained with reference to published evidence on the Laptev Sea (Bauch et al., 2001), and the glacial one was calculated according to data on isostatic subsidence and uplift during glaciation and deglaciation, respectively (Ushakov and Krass, 1972; Nikonov, 1977; Bylinsky, 1996). Figure 4 shows that the calculations for the glacial domain were made taking into account (I) the thickness of the MIS-2 ice sheet (rising 500 m above the sea bottom subsidence under the ice load; the fall reached 140 m, or 20 m below the global average regression limit (Lambeck and Chappell, 2001).

In postglacial times, the sealevel rose during transgression in the periglacial domain but fell in the glacial one as a result of Novaya Zemlya uplift. Thus, the glacial domain was exposed to weaker cooling during the glacial period and became flooded and exposed to permafrost degradation right after ice melting. Unlike this, flooding in the periglacial domain was accompanied by permafrost degradation for as long as 1500 years.

The construction of scenarios of rock temperature dynamics by the authors during the estimated time is the final part of the paleogeographic materials for the conduction of the numerical modeling. The ground temperatures were reconstructed in several 1D solutions, with reference to paleo-water chemistry (Fotiev, 1999; Volkov, 2006) and oxygen isotope composition of ice wedges (IW, $\delta^{18}\text{O}_{\text{IW}}$) (Vasil'chuk, 1992), as well as to reconstructed summer air temperatures. The $\delta^{18}\text{O}_{\text{IW}}$ data were corrected according to the results of Golubev et al. (2001).

We present the paleogeographic scenario as a series of paleotemperature curves adapted to the modeling purposes (Figs. 5, 7). Altogether thirty such curves have been obtained, each based on four lithological patterns and two heat flux values.

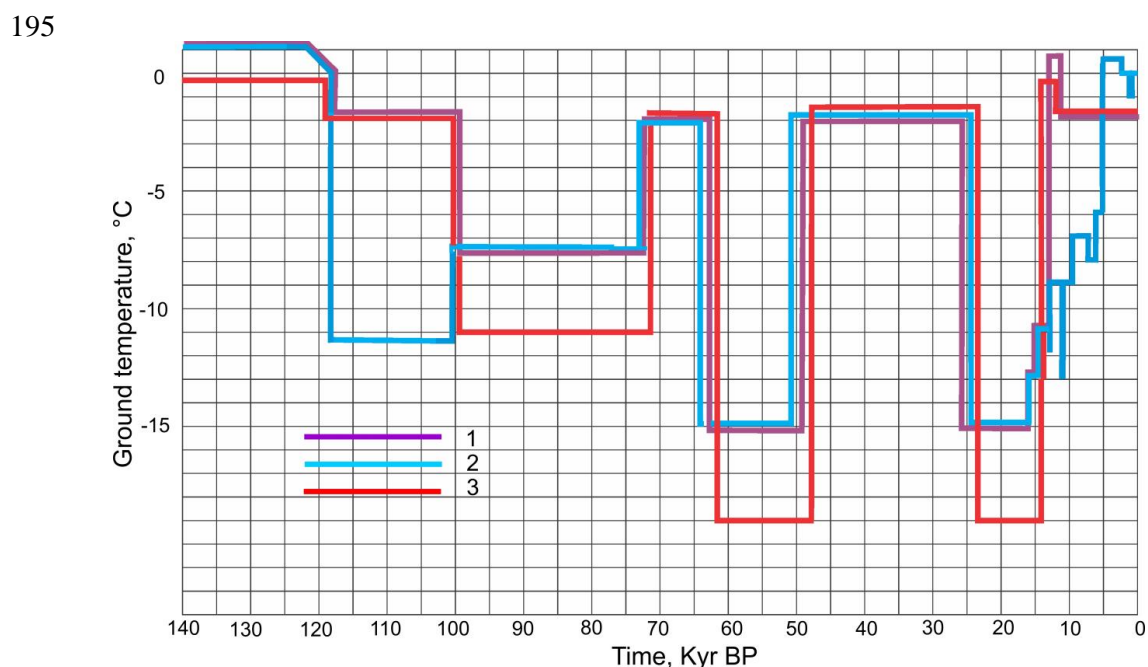


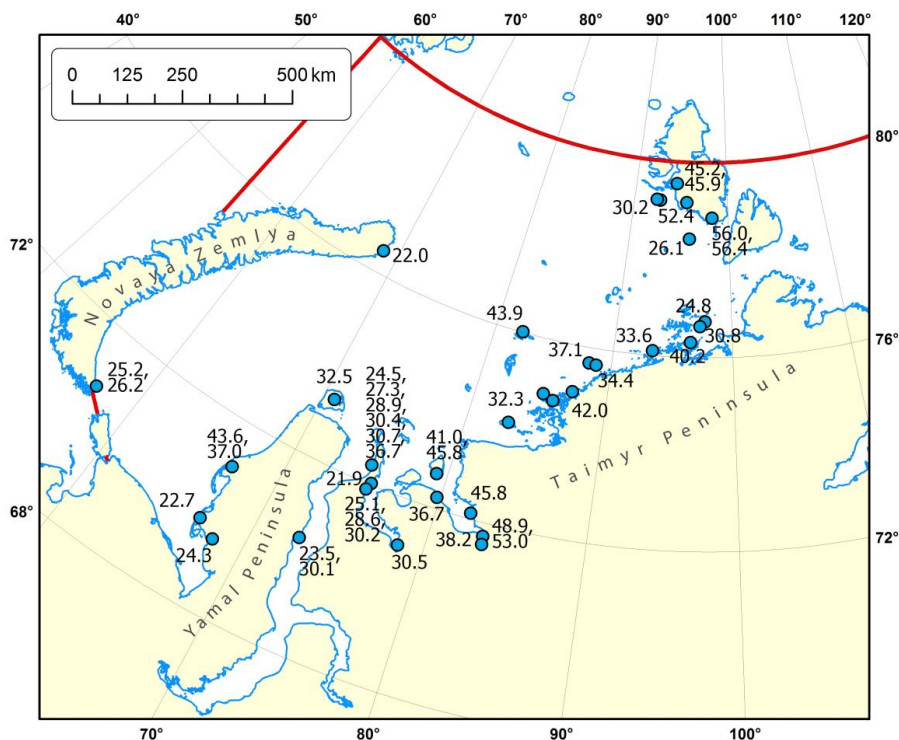
Fig. 5. Paleo-temperature for the periglacial subaerial part of the shelf:
1 = southwestern shelf part (SW), 80 m isobath; 2 = southwestern shelf part (SW), 5 m isobath;
3 = northeastern shelf part (NE), 120 m isobath.

During transgressions in the Holocene, each shelf part stayed for 400-2000 years in the coastal zone where bottom sediments were flooded with saline and warm near-bottom water.



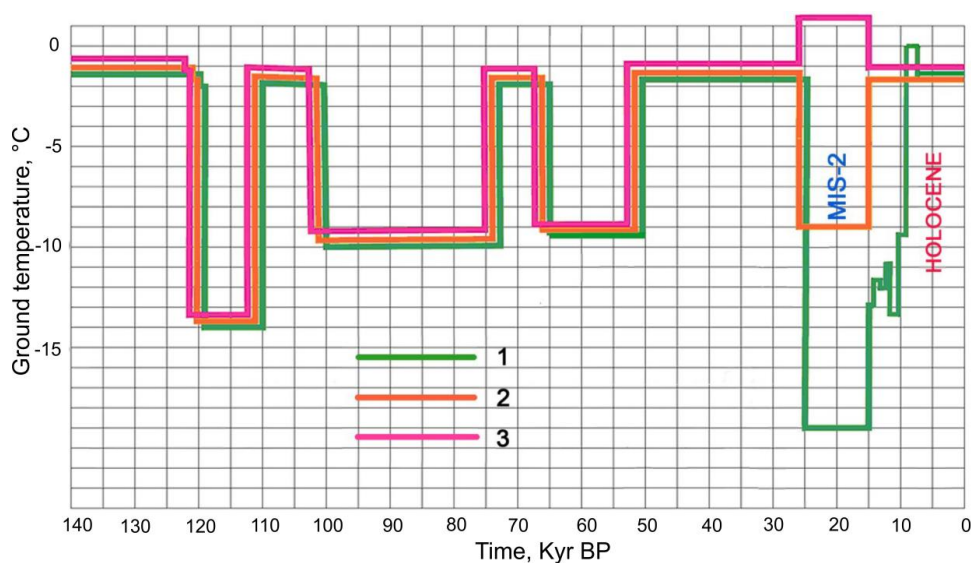
205 The scenarios record alternated cold and warm events accompanied, respectively, by regressions and transgressions (Figs. 5, 7), which created conditions for permafrost growth and degradation. At glaciation peaks, the present sea bottom in the periglacial shelf part was above the shores which subsided under the ice load. This led to the formation of marine terraces, i.e., the sea level fall during cold events (MIS-5b, MIS-4) was smaller than the global average.

210 The available data, though far incomplete, show that the sea level between 50 and 25 Kyr BP (almost all MIS-3 through) was the same as at present (Fig. 6), in our opinion it is also due to post-Zyryanian uplift (isostatic rebound). On the other hand, the current state of permafrost has been controlled by the ground temperature in the periglacial shelf part and by the presence of an ice-dammed freshwater basin (Fig. 7). In the Holocene, the effect of >0 °C bottom water in the near-shore zone during warm climate events was critical for permafrost degradation from above (Figs. 5, 7). The MIS-2 ground temperature in the glacial shelf part was warmer (Fig. 7, the curve 2) due to thermal insulation by ice.



215

Fig. 6. Location of onshore and offshore sections (points) with marine sediments (^{14}C - figures, thousand years ago) of MIS-3 in the Kara Sea shelf, after Gusev et al. (2011; 2012a, b; 2013a, b; 2016 a, b); Baranskaya et al. (2016); Vasil'chuk et al. (1984); Molodkov et al. (1987); Bolshiyarov et al. (2009).



220

Fig. 7. Paleogeographic scenario for MIS-2 which controlled the present distribution of frozen and cold ground. Adapted for modeling purposes. A fragment.

1 = periglacial subaerial northeastern shelf part (NE); 2 = ice that reached the bottom for 7-10 kyr, G-1); 3 = subaqual (beneath damlake) central shelf part, C;

225

4. Simulation results and regional interpretation

The simulation results show that the distribution of strata of rocks that differ in their state (thawed, cooled, frozen) are associated with the paleogeographic events of the Late Pleistocene-Holocene. In the distribution of permafrost, a particularly close relationship occurs with glaciation in the MIS-2, the glacier and the Holocene optimum.

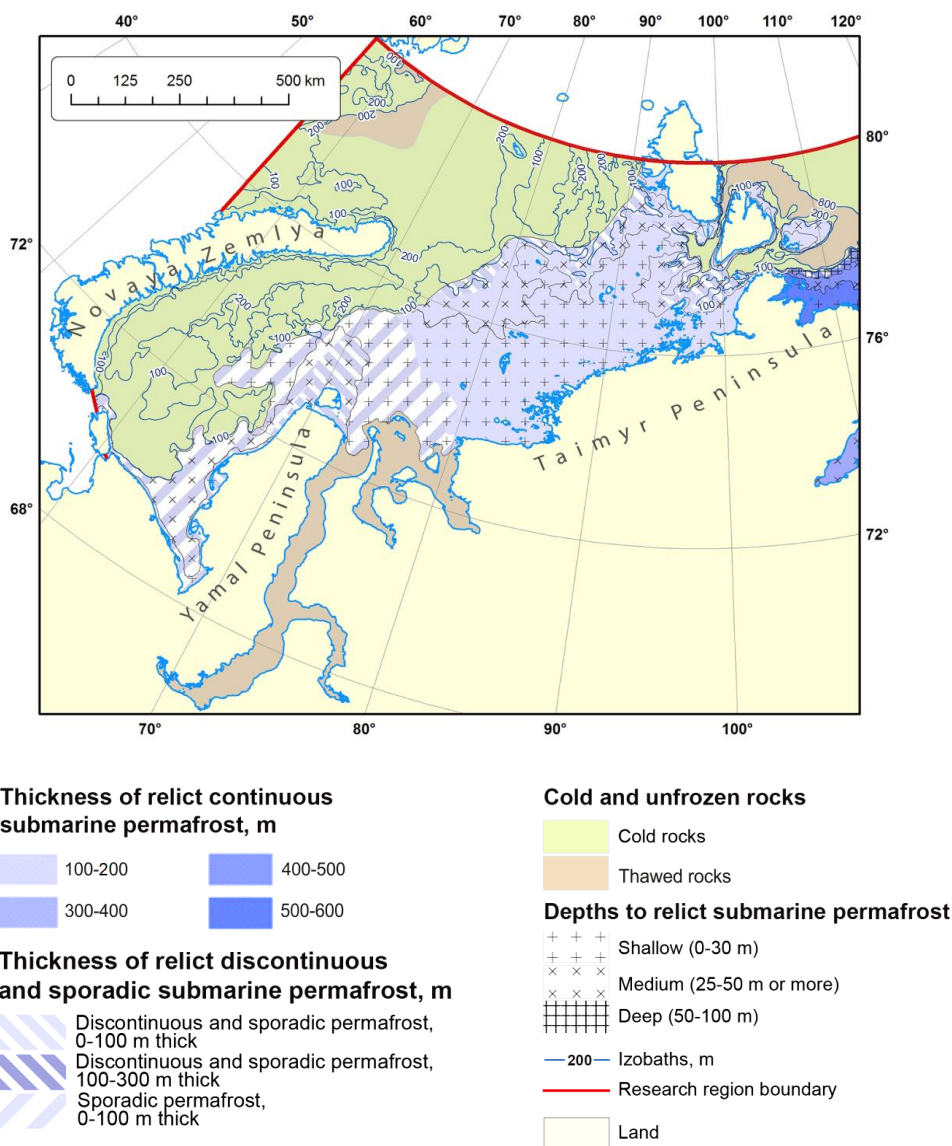
230

4.1. Distribution of frozen, cold, and unfrozen rocks

Permafrost occurs within the areas that were free from MIS-2 ice sheets (SW, NE, C and partly E in Fig. 3; Figs. 8, 9, 10). The present areas of cold ground were covered with ice that reached the sea bottom during MIS-2 (Fig. 3). Unfrozen rocks occupy the areas which were open to the input of >0 °C Atlantic waters (Levitan et al., 2009) in early postglacial time (16-15 Kyr BP): a part of the G-2 zone (Fig. 3) and a large part of estuaries (E in Fig. 3), except for their northern ends.

235

Frozen ground is restricted to the periglacial domain. The boundary between the periglacial and glacial domains and, correspondingly, between the unfrozen and frozen or cold ground is delineated by the limits of MIS-2 ice that reached the sea bottom and remained in contact with it for 7-10 thousands of years (Fig. 3), and by the 120 m isobath in the northeastern shelf part, within Severnaya Zemlya and the Cheluskin Peninsula (Figs. 3, 8).



240

Fig. 8. Fragments of the map of the permafrost zoning of the Kara Sea and the legend.

4.2. Distribution of permafrost, its thickness and depth to the top

245

Permafrost becomes more extensive, shallower and thicker from southwest to northeast and from deep offshore toward near-shore shallow waters. This pattern has several controls:

- (1) latitudinal climatic zonation and division into sectors;
- (2) sea depths that affect the duration of shelf drying and flooding (permafrost formation and degradation, respectively);

250

- (3) ice-dammed freshwater basin in MIS-2;
- (4) deep heat flux;



- (5) lithology and properties of rocks;
- (6) sea water and seasonal ice cover (salinity and freezing-thawing temperatures of rocks);
- (7) thermal effect of river waters;
- 255 (8) Holocene climate optimum.

The southwestern part of the Kara Sea experienced an impact of warm water inputs (Pogodina, 2009) in the middle Holocene (the Holocene optimum), judging by the distribution of thermophile foraminifera communities with predominant Arctic-boreal species found currently in the Pechora Sea. Therefore, the >0 °C bottom water temperatures common to the present-day Pechora Sea may have existed 7-5 Kyr BP in the southwestern Kara shelf and provided thawing of permafrost from above.

The distribution of permafrost also depends on deep heat flux which may reach 50-60 mW/m² over the greatest part of the Kara shelf (Khutorskoi et al., 2013). Temperature logs from deep boreholes in the shelf and coastal gas reservoirs of Yamal give heat flux values of 73-76 mW/m². Other controls include lithology, water contents, physical properties, and salinity (freezing-thawing temperatures) of rocks.

Tables 2 and 3 lists the most common depths to the permafrost table determined in previous studies and according to our own calculations. They may vary significantly, even within marine geosystems of the same type: according to drilling results, they are 56 m in the near-shore zone at the Kharasavei Cape and as shallow as 5 m in the Sharapov Shar Gulf 50-60 km in the south. The prospective values are 30-40 m below the sea bottom under the Yamal shores and close to the water table under the retreating coast (Baulin et al., 2005). The permafrost thickness was estimated as the difference between the depths to permafrost top and base

4.2.1. Southwestern periglacial shelf

The southwestern part of the Kara shelf (SW in Fig. 3) is occupied by discontinuous and sporadic permafrost (Fig. 8), as inferred from modeling with reference to field data (Dlugach and Antonenko, 1996; Melnikov and Spesivtsev, 1995; Baulin, 2001; Bondarev et al., 2001; Rokos et al., 2001, 2007, 2009; Baulin et al., 2005; Neizvestnov et al., 2005; Kulikov and Rokos, 2017). According to the modeling results, permafrost can exist in sand at a heat flux of 50 mW/m² but is absent in all other lithologies at 75 mW/m² (Table 2).



280

Table 2. Modeling results for depths to permafrost top and base and permafrost thickness, uniform lithology, SW

area

| Sea depth, m | Lithology | Heat flux from below, mW/m ² | | | | | |
|-----------------|-----------|---|--------------------|--------------|---------------------|--------------------|---------------|
| | | 50 | | | 75 | | |
| | | Depth to base, m | Depth to top, m | Thickness, m | Depth to base, m | Depth to top, m | Thickness*, m |
| 5 | sand | 190 | 50 | 140 | 175 | 55 | 120 |
| | clay silt | 110 | 45 | 65 | 0 | | |
| | bedrock | 150 | 45 | 105 | 0 | | |
| 20 | sand | 180 | 50 | 130 | 140 | 60 | 80 |
| | clay silt | 75 | 40 | 35 | 0 | | |
| 50 | sand | 175 | 50 | 125 | 130 | 60 | 70 |
| | clay silt | 0 | | | 0 | | |
| | bedrock | 120 | 60 | 60 | 0 | | |
| 80 | sand | 165 | 65 | 100 | 82 | 55 | 27 |
| 120 | sand | 0 | | | 0 | | |
| | clay silt | 0 | | | 0 | | |
| | bedrock | 0 | | | 0 | | |

*the quoted permafrost thicknesses in all tables here and below are current residual values.



285

Table 3. Modeling results for depths to permafrost top and base and permafrost thickness, alternated sand and clay silt (clay), SW area

| Sea depth, m | Layered sequence, 0.5 and 0.3 volumetric fraction of sand (n_n) | Heat flux from below, mW/m^2 | | | | | |
|--------------|---|---------------------------------------|-----------------|--------------|------------------|-----------------|--------------|
| | | 50 | | | 75 | | |
| | | Depth to base, m | Depth to top, m | Thickness, m | Depth to base, m | Depth to top, m | Thickness, m |
| 5 | $n_n=0.5$ | 133 | 40 | 93 | 0 | | |
| | $n_n=0.3$ | 117 | 40 | 77 | 0 | | |
| 50 | $n_n=0.5$ | 132 | 50 | 82 | 0 | | |
| | $n_n=0.3$ | 124 | 55 | 69 | 0 | | |
| 120 | $n_n=0.5$ | 0 | | | 0 | | |
| | $n_n=0.3$ | 0 | | | 0 | | |



Table 4. Modeling results for depths to permafrost top and base and permafrost thickness, 50 m of alternated sand and clay silt (clay) lying over bedrock, SW area

| Sea depth, m | Layered sequence, 0.5 and 0.3 volumetric fraction of sand (n_s) | Heat flux from below, mW/m^2 | | | | | |
|--------------|---|---------------------------------------|-----------------|--------------|------------------|-----------------|--------------|
| | | 50 | | | 75 | | |
| | | Depth to base, m | Depth to top, m | Thickness, m | Depth to base, m | Depth to top, m | Thickness, m |
| 5 | $n_s=0.5$ | 129 | 40 | 89 | 0 | | |
| | $n_s=0.3$ | 115 | 40 | 75 | 0 | | |
| 50 | $n_s=0.5$ | 130 | 55 | 75 | 0 | | |
| | $n_s=0.3$ | 127 | 57 | 70 | 0 | | |
| 120 | $n_s=0.5$ | 0 | | | 0 | | |
| | $n_s=0.3$ | 0 | | | 0 | | |

290



295 The quantitative modeling results show (Table 2) that the permafrost state depends on lithology if it is uniform. However, the real shelf sections (e.g., in boreholes of the Leningradskaya and Rusanovskaya fields) consist of different alternating lithologies. Therefore, data listed in Table 2 are applicable uniquely as a check for the role of lithology and rock properties in the formation, distribution and thickness of permafrost, and in depths to its top and base, which were estimated for layered sections.

300 Along the west coast of the Yamal Peninsula (area of the Kharasavei-Sea field), where the modern frozen rocks make up the upper part of the section, and their relic rocks are underlain, permafrost in the Kharasavei shelf gas and condensate deposit forms three elongate zones: ~0.5 km wide zone of continuous permafrost near the shore (0-2 m sea depth); discontinuous permafrost, 1-3 km wide, sea depths to 5-7 m (Baulin, 2001; Baulin et al., 2005); and sporadic permafrost, which may spread to sea depths of 80 m (our estimate), or 100 m (Kulikov and Rokos, 2017) to 105 m (Vasiliev et al., 2018).

305 The depths to the permafrost table are variable, especially near the shore, as a result of coastal advance and retreat. Permafrost currently exists in zones of coast aggradation, while permafrost beneath retreating coasts is the shallowest at the shoreline and becomes deeper seaward. Specifically, permafrost was stripped at a depth of 0.5 m below the sea bottom at the geocryological site Marre-Sale, in borehole 16-14 drilled for temperature monitoring 0.5 km far from a retreating coast (Dubrovin et al., 2015) but is deeper (3.5 m) in another monitoring borehole 15-14 located 0.9 km far from the shore, where a 0°C mean annual ground temperature was recorded at 3 m subbottom depth. On the other hand, the permafrost table beneath stable coast may be as deep as 30-50 m (Baulin et al., 2005). Similar depth variations occurred also during the Holocene transgression, i.e., this is a typical feature of local permafrost. However, generally the depths to permafrost increase offshore and depend on its composition and ice content, as well as on the time when it submerged.

310 Within the sea depths from 2 to 5-7 m, the depth to permafrost varies from 5 to 30-40 m. Similar values were inferred by modeling for the most realistic sections of interbedded sand and clay (40 m at a heat flux of 50 mW/m²). The calculated most probable permafrost thickness for these lithologies is 75-90 m at 50 mW/m². It agrees with 60-80 m reported by Badu (2014) as well as with the estimates 90 m and 70 m by Vasiliev (2018) for the sea depths about 10 m and 35 m, respectively. Permafrost in terrace I of Yamal, which formed from MIS-2 through the Holocene and was not exposed to prolonged subsea degradation, is as thick as 185 m (Trofimov et al., 1975; Yershov, 1989).

315 According to calculations, on isobaths exceeding 7-10 m, the subsea permafrost table is as deep as 50-80 m (Table 3), which agrees with estimates based on field data (Melnikov and Spesivtsev, 1995). It is most likely beyond the reach of engineering geological drilling (Baulin et al., 2005).

320 Permafrost is discontinuous to sporadic closer to the shore and sporadic at greater sea depths, with the boundary at the 10 m isobath. The depths to permafrost table are 0-30 in two first zones and 20-50 m in the offshore zone. The permafrost thickness is from 0 to 100 m (Fig. 8).

325 Similar distribution and parameters of permafrost are common to other parts of the southwestern periglacial shelf, but they vary slightly as a function of zonal features. Farther in the north, the boundary between discontinuous and sporadic permafrost follows the 20 m isobath. The depths to the permafrost table are 30 to 70 m at sea depths from 0 to 20 m according to field data, and 40 to 70 m according to calculations; the calculated permafrost thickness is mainly <100 m (the estimates in Table 2 are for reference sections and those in Tables 3-4 are real data). In real sections within 20-80 m sea depths, permafrost lies at a depth of 50-55 m and is 70-90 m thick (Tables 3-4).

330 The permafrost changes from discontinuous to sporadic below the 5 m sea depth south of the Kharasavei deposit and is only sporadic still farther to the south (end of the Baidaratskaya Guba Bay).



4.2.2. *Northeastern periglacial shelf*

335 There is no drilling data for this shelf part (NE in Fig. 3; Fig. 8). According to logs from a test well in Sverdrup Island, heat flux, varies from 25 to 60 mW/m² as a function of lithology and thermal properties of rocks at different core depths (Khutorskoi et al., 2013). Modeling results for a heat flux of 50 mW/m² predict that the permafrost is continuous at sea depths within 0-80 m and discontinuous to sporadic from 80 to 120 m (Tables 5-7). Cold rocks may exist at these sea depths mainly in clay sediments, at different heat flux values, though permafrost is predominant (Tables 5-7).

340



Table 5. Modeling results for depths to permafrost top and base and permafrost thickness, uniform lithology, NE area

| Sea depth, m | Lithology | Heat flux from below, mW/m ² | | | | | |
|-----------------|-----------|---|--------------------|--------------|---------------------|--------------------|--------------|
| | | 50 | | | 75 | | |
| | | Depth to base, m | Depth to top, m | Thickness, m | Depth to base, m | Depth to top, m | Thickness, m |
| 5 | sand | 270 | 25 | 245 | 175 | 25 | 150 |
| | clay silt | 130 | 20 | 110 | 0 | | |
| | bedrock | 190 | 28 | 162 | 0 | | |
| 20 | sand | 260 | 30 | 230 | 160 | 32 | 128 |
| 50 | sand | 250 | 35 | 215 | 150 | 35 | 115 |
| | clay silt | 120 | 35 | 85 | 0 | | |
| | bedrock | 170 | 40 | 130 | 0 | | |
| 80 | sand | 230 | 40 | 190 | 105 | 40 | 62 |
| 120 | sand | 212 | 50 | 162 | 85 | 50 | 35 |
| | clay silt | 0 | | | 0 | | |
| | bedrock | 90 | 50 | 40 | 0 | | |



345

Table 6. Modeling results for depths to permafrost top and base and permafrost thickness, alternated sand and clay silt (clay), NE area

| Sea depth, m | Layered sequence, 0.5 and 0.3 volumetric fraction of sand (n_n) | Heat flux from below, mW/m^2 | | | | | |
|-----------------|--|---------------------------------------|--------------------|--------------|---------------------|--------------------|--------------|
| | | 50 | | | 75 | | |
| | | Depth to base, m | Depth to top, m | Thickness, m | Depth to base, m | Depth to top, m | Thickness, m |
| 5 | $n_n=0.5$ | 221 | 20 | 201 | 107 | 20 | 87 |
| | $n_n=0.3$ | 190 | 20 | 170 | 75 | 20 | 55 |
| 50 | $n_n=0.5$ | 206 | 35 | 171 | 91 | 38 | 53 |
| | $n_n=0.3$ | 171 | 35 | 136 | 61 | 37 | 24 |
| 120 | $n_n=0.5$ | 121 | 45 | 76 | 0 | | |
| | $n_n=0.3$ | 85 | 40 | 45 | 0 | | |



350

Table 7. Modeling results for depths to permafrost top and base and permafrost thickness, 50 m of alternated sand and clay silt (clay) lying over bedrock, NE area

| Sea depth, m | Layered sequence, 0.5 and 0.3 volumetric fraction of sand (n_n) | Heat flux from below, mW/m ² | | | | | |
|-----------------|--|---|--------------------|--------------|---------------------|--------------------|--------------|
| | | 50 | | | 75 | | |
| | | Depth to base, m | Depth to top, m | Thickness, m | Depth to base, m | Depth to top, m | Thickness, m |
| 5 | $n_n=0.5$ | 214 | 21 | 193 | 0 | | |
| | $n_n=0.3$ | 208 | 21 | 187 | 0 | | |
| 50 | $n_n=0.5$ | 195 | 37 | 158 | 0 | | |
| | $n_n=0.3$ | 188 | 36 | 152 | 0 | | |
| 120 | $n_n=0.5$ | 103 | 43 | 60 | 0 | | |
| | $n_n=0.3$ | 95 | 40 | 55 | 0 | | |



355 The depth to the top of continuous permafrost is most often from 20-25 m near the shore to 35-40 m at sea depths
50-80 m (Table 6). The permafrost thickness varies from 150 to 200 m in sand-clay sediments depending on lithology and
sea depth. Correspondingly, the map of Fig. 8 shows typical depths to permafrost in a range of 0 to 30 m and permafrost
thicknesses from 100 to 200 m. Discontinuous permafrost lies at a depth of 40-45 m and is 0 to 100 m thick.

4.2.3. Central area

360 The central area covers the offshore extension of the Ob', Yenisey, and Gyda rivers (C in Fig. 3; Fig. 8) in the
middle between the southwestern shelf part from the northeastern one. The area was interpreted (Kulikov and Rokos, 2017)
as an unfrozen zone (a talik) corresponding to paleo-estuaries and paleo-deltas of the West Siberian rivers. In our view,
however, it was rather a lake-like freshwater basin that formed when ice dammed the continuing flow of the large Siberian
rivers (Ob, Yenisei, Taz, etc.) during the MIS-2 glacial event. The ice dam caused flooding of the respective shelf part in
365 different periods; the surface area and elevations of the lake table (C in Fig. 3) changed accordingly with the ice sheet
contours. Therefore, our map delineates the lake by isobaths from 0 to 80 m.

The Central area is shown in the map as occupied by sporadic permafrost: sea bottom rises within its limits may be
frozen (like the cases of Yamal and Ob' Gulf). In fact, permafrost patches beneath the Sartan damlake are scarce as the
rocks had stored large heat resources while staying under the ice sheet for thousands of years. The sediments currently
370 occurring within the lake limits were much warmer than the surrounding rocks during MIS-2: +4 °C against -19 to -23 °C,
respectively. The patches of permafrost lie at depths from 0 to 30 m and the permafrost thickness is a few tens of meters.

4.2.4. Estuary (bays)

375 Permafrost in the quite well documented Ob' estuary (E in Fig. 3) is restricted to a narrow strip along the shore; it
is relict permafrost beneath the coast exposed to marine erosion. The total thickness of present and relict permafrost
exceeds 20 m within the 1 m isobath, is no more than 10 m at sea depths between 0 and 2-3 m, and pinches out seaward in
deeper water; the depth to subsea permafrost within 3 m of water depths is 5 to 15 m or more (Baulin, 2001). Coastal
permafrost is traceable as far as the Cape Kamenny at 68°N (Kokin and Tsvetinsky, 2013). The patches of frozen ground
are limited to a 100 m wide strip along the shore (less often 300 m).

380 Seismic reflection profiling reveals numerous gas reservoir zones (Rokos and Tarasov, 2007) and presumably a
frozen rock mass at a sea depth of 15 m at 71° N (Slichenkov et al., 2009). The estuaries (south of 71.5° N) are mapped as
mainly unfrozen zones with near-shore permafrost at ≤ 3 m sea depths.

We agree with the previous inference (Melnikov et al., 1998; Badu, 2014, etc.) that permafrost within gas fields
(Rusanovskaya and other gas-bearing geological structures) refers to relict frozen rocks. Their genesis and cryogenic
385 age is the subject of debate.

5. Conclusions

390 The present state and 125 Kyr history of permafrost in the Kara shelf has been modeled with reference to the
existing knowledge. Since 125 Kyr ago, the parameters of permafrost have been controlled by glacial and isostatic rebound
events: frozen ground is present currently in places which were free from ice but is absent from those covered by ice during
the MIS-2 glacial.

Degradation of glaciation led to ice rebound and related transgression. As a result, permafrost thawed, partially
after the MIS-5b cold event and completely after the MIS-4 event (during the Karginian interstadial, MIS-3).

395 As a result, the present shelf comprises frozen, cold, and unfrozen rocks. Permafrost occurs in the periglacial
domain, cold rocks correspond to areas of MIS-2 glaciation, while unfrozen rocks occupy the areas that were exposed to



the effect of >0 °C Atlantic waters (e.g., the western St. Anna trench) in the early postglacial time (16-15 Kyr BP); unfrozen rocks are also found over the overwhelming part of river estuaries in northern West Siberia, except for the river mouths.

400 The periglacial shelf part is divided into zones of continuous, discontinuous to sporadic, and sporadic permafrost. The geocryological conditions become harsher (continuous, deep, and thick permafrost) from southwest to northeast and from large sea depths to near-shore shallow water.

The distribution and parameters of permafrost have had multiple controls:

- 405 (1) latitudinal climatic zonation and division into sectors;
(2) sea depths that affected the duration of regressions and transgressions and the related freezing and thawing of permafrost, respectively;
(3) an ice-dammed freshwater lake that existed during the MIS-2 event;
(4) deep heat flux;
(5) lithology and properties of rocks;
(6) sea water and seasonal ice cover that affect salinity (and hence freezing-thawing temperatures) of sediments;
410 (7) thermal effect from river waters.

The periglacial shelf part is divided into the southwestern, northeastern, central, and estuary areas. The southwestern area comprises two subareas: a zone of discontinuous to sporadic permafrost along the shore, within 20 m sea depths in the north and 5-7 m in the south, which grades seaward into a zone of only sporadic permafrost. In the former zone, the permafrost has its table at depths from 0 to 30 m and is a few tens of meters to 100 m thick; in the latter zones, the
415 depth to permafrost is 20 to 50 m and the permafrost thickness is less than 50 m.

In the northeastern area, continuous permafrost occurs within sea depths from 0 to 80 m and has a thickness of 100-200 m; the depth to its top varies from 0 to 30 m. The 80-120 m sea depth interval is occupied by ≤ 100 m thick discontinuous to sporadic permafrost with its table at a depth of 20-50 m.

420 Permafrost in the central area is sporadic; it is within 50 m thick and its top lies from 0 to 30 m deep. Rocks in the estuaries are mostly unfrozen; relict permafrost is restricted to a 100-300 m strip along the shore.

The studies performed were based on drilling and seismic acoustic data published to date. The study of the shelf by drilling and geophysical methods continues. Therefore, the results of the studies performed by the authors can be used in planning new drilling and in the geocryological interpretation of seismoacoustic profiling.

425 **Acknowledgement**

The authors are grateful to all project participants in the for assistance in collecting and processing an extensive amount of information from various fields of knowledge that was necessary for conducting the research and obtaining the presented results. The project was carried out by the Foundation «National Intellectual Resource» (involving experts from Moscow State University) jointly with the Arctic Research Center of the Rosneft Oil Company.

430

References

- Astakhov V.I., Nazarov D.V.: Late Pleistocene stratigraphy in northern West Siberia. *Regionalnaya Geologiya i Metallogeniya*, 43, 36-47, 2010.
- 435 Badu Yu. B.: The influence of gasbearing structures on the thickness of cryogenic strata of Jamal Peninsula. *Kriosfera Zemli*, XVIII (3), 11-22, 2014.



- Baranov I.Ya.: Geocryological Map of the USSR. Scale 1:10 000 000. Explanatory Note. Moscow, 48 pp, 1960 (in Russian).
- 440 Baranskaya A.V., Romanenko F.A., Arslanov Kh.A., Maksimov F.E., Starikova A.A. and Pushina Z.V.: Perennially frozen deposits of Bely island: stratigraphy, age, depositional environments. *Earth's Cryosphere*, XXII (2), 3-15, 2018.
- Bauch H.A., Muller-Lupp T., Taldenkova E., Spielhagen R.F., Kassens H., Grootes P.M., Thiede J., Heinmeier J., Petryasov V.V.: Chronology of the Holocene transgression at the Northern Siberia margin. *Global and Planetary Change*, 31 (1-4), 125-139, 2001.
- 445 Baulin V.V.: Engineering geological studies in the Arctic shelf: experience, results, and regulations, in: Development of the Russian Arctic Shelf, Proc. 5th Intern. Conf. RAO-01, St. Petersburg, 36-239, 2001 (in Russian).
- Baulin V.V., Ivanova N.V., Rivkin F.M., Chernyad'ev V.P., Shamanova I.I.: Coastal cryolithozone of the Northwest Yamal: problems of development. *Kriosfera Zemli*, IX (1), 28-37, 2005.
- Bolsiyarov D.Y., Anokhin V.M., Gusev E.A.: New data on the structure of the relief and the fourth vertical deposits of the Novaya Zemlya archipelago // Geological and geophysical characteristics of the lithosphere of the Arctic region. SPb, VNIIOkeangeologiya, Proceedings of VNIIOkeangeologiya, vol. 210, Issue 6, 149-161, 2006
- 450 Bolshiyarov D.Y., Grigoriev M.N., Schneider V., Makarov A.S., Gusev E.A.: Late Pleistocene sealevel change and formation of an ice complex on the Laptev Sea shore, in: Basic Problems of the Quaternary: Results and Main Prospects, Geos, Moscow, 45-49, 2007 (in Russian).
- Bolshiyarov D.Yu., Pogodina I.A., Gusev E.A., Sharin V.V., Aleksev V.V., Dymov V.A., Anohin V.A., Anikina N.Yu., 455 Derevyanko L.G.: Shorelines of the Franz Joseph Land, Novaya Zemlya, and Svalbard: New data. *Problemy Arktiki i Antarktiki* 82 (2), 68-77, 2009.
- Bondarev V.N., Loktev A.S., Dlugach A.G., Potapkin Yu.V.: Methods for studies of subsea permafrost, in: Sedimentological Processes and Evolution of Marine Ecosystems in Marine Periglacial Conditions, Book 1, Apatity, 15-19, 2001 (in Russian).
- 460 Bylinskiy E.N.: Effect of Glacial Isostasy on the Pleistocene Terrane Evolution. National Geophysical Committee of the Russian Academy of Sciences, Moscow, 212 pp, 1996. (in Russian)
- Chekhovsky A.L.: Distribution of permafrost under the Kara Sea bottom. *Transactions, PNIIS*, Moscow, Issue 18, 100-110, 1972.
- Danilov I.D., Buldovich S.N.: Dynamics of permafrost related to transgressions and regressions in the Arctic basin, in: 465 Fundamentals of Geocryology, Book 4, Moscow State University, Moscow, 372-382, 2001 (in Russian).
- Derevyagin A.Yu., Chizhov A.B., Brezgunov V.S., Hubberten Kh.-V., Siebert K.: Stable isotope composition of ice wedges in the Sabler Cape (Lake Taimyr). *Kriosfera Zemli*, III (3), 41-49, 1999.
- Dlugach A.G., Antonenko S.V.: Main Distribution and Structure Patterns of Permafrost in the Barents-Kara Shelf: Implications for Petroleum Exploration. AMIGE, Murmansk, 271 pp, 1996 (in Russian).
- 470 Dubrovin V.A., Kritsuk L.N., Polyakova E.I.: Temperature, composition and age of the Kara sea shelf sediments in the area of the geocryological station Marre-Sale. *Earth's Cryosphere*, XIX (4), 3-16, 2015.
- Forman S.L., Ingolfsson O., Gataullin V., Manley W., Lockrantz H.: Late Quaternary stratigraphy, glacial limits, and paleoenvironments of the Marresale area, western Yamal Peninsula, Russia. *Quaternary Research*, 57, 355-370 pp., 2002.
- Fotiev S.M.: Formation of the major-ion chemistry of natural waters in the Yamal Peninsula. *Kriosfera Zemli*, III (2), 40-475 65, 1999.
- Gavrilov A.V.: The cryolithozone of the Arctic shelf of Eastern Siberia (current state and history of development in the Middle Pleistocene - Holocene). *Dissertation for a degree. D.Sc. M.*, 2008, 48 pp.



- Geinz A.E., Garutt V.E.: Radiocarbon (^{14}C) dating of mammoth and woolly rhinoceros fossils from Siberian permafrost. *Doklady Akademii Nauk*, 154 (6), 1367- 1370, 1964.
- 480 Gilbert M.Th.P., Tomsho L.P., Rendulic S., Packard M., Drautz D.I., Sher A., Tikhonov A., Dalen L., Kuznetsova T., Kosintsev P., Campos P.F., Higham Th, Collins M.J., Wilson A.S., Shidlovskiy F., Buigues B., Ericson P.G.P., Germonpre M., Gotherstrom A., Iacumin P., Nikolaev V., Nowak-Kemp M., Willerslev E., Knight J.R., Irzyk G.P., Perbost C.S., Fredrikson K.M., Harkins T.T., Sheridan Sh, Miller W., Schuster S.C.: Whole-genome shotgun sequencing of mitochondria from ancient hair shafts. *Science*, 317, 1927–1930, 2007.
- 485 Flint R.F.: *Glacial and Pleistocene geology*. N.Y., J. Wiley a. sons, 553 pp., 1957
- Gavrilov A.V., Romanovskii N.N., Romanovsky V.E. and Hubberten H.-W.: Offshore Permafrost Distribution and Thickness in the Eastern Region of Russian Arctic In: "Changes in the Atmosphere-Land-Sea System in the American Arctic". Proceedings of the Arctic Regional Centre. Volum 3. Edited by Igor P. Semiletov. Dalnauka, Vladivostok, 209-218, 2001.
- 490 Golubev V.N., Konishchev V.N., Sokratov S.A., Grebennikov P.B.: The effect of seasonal snow sublimation on the oxygen isotope composition of ice wedges. *Kriosfera Zemli*, 3, 71-77, 2001.
- Grigoriev N.F.: Coastal Permafrost in the Western Yamal Peninsula. Kn. Izdatelstvo, Yakutsk, 110 pp, 1987 (in Russian).
- Gusev E.A., Arslanov Kh.A., Maksimov F.E., Molod'kov A.N., Kuznetsov V.Yu., Smirnov S.B., Chernov S.B., Zherebtsov I.E., Levchenko S.B.: Late Pleistocene-Holocene sediments in the Yensei lower reaches: New geochronological data. *Problemy Arktiki i Antarktiki*, 2 (88), 36-44, 2011.
- 495 Gusev E.A., Sharin V.V., Dymov V.A., Kachurina N.V., Arslanov Kh.A.: Shallow sediments in the northern Kara shelf: New data. *Razvedka i Okhrana Nedr* 8, 87-90, 2012a.
- Gusev E.A., Kostin D.A., Rekant P.V.: Genesis of Quaternary deposits in the Barentsevo-Kara shelf (State Geological Map of the Russian Federation, scale 1:1 000 000). *Otechestvennaya Geologiya*, 2, 84-89, 2012b.
- 500 Gusev E.A., Bolshiyarov D.Yu., Dymov V.A., Sharin V.V., Arslanov Kh.A.: Holocene marine terraces of southern islands of the Franz Joseph Land archipelago. *Problemy Arktiki i Antarktiki*, 97 (3), 103-108, 2013a.
- Gusev E.A., Anikina N.Yu., Arslanov Kh.A., Bondarenko S.A., Derevyanko L.G., Molod'kov A.N., Pushina Z.V., Rekant P.V., Stepanova G.V.: Quaternary stratigraphy and pleogeography in Sibiryakov Island for the past 50 000 years. *Proceedings of the Russian Geographical Society*, 145 (4), 65-79, 2013b.
- 505 Gusev E.A., Molodkov A.N., Anikina N.Yu., Derevyanko L.G.: Origin and age of watershed sands in the northern part of the Yenisei catchment. *Proceedings of the Russian Geographical Society*, 147 (4), 51-62, 2015a.
- Gusev E.A., Molodkov A.N., Derevyanko L.G.: The Sopkarga mammoth, its age and living conditions (northern West Siberia). *Uspekhi Sovremennogo Estestvoznaniya* 1-3, 432-435, 2015b.
- Gusev E.A., Maksimov F.E., Molodkov A.N., Yarzhembovsky Ya.D., Makaryev A.A., Arslanov Kh.A., Kuznetsov V.Yu., Petrov A.Yu., Grigoryev V.A., Tokarev I.V.: Late Pleistocene-Holocene deposits of western Tai'myr and islands of the Kara Sea: New geochronological constraints. *Problemy Arktiki i Antarktiki*, 109(3), 74-84, 2016a.
- Gusev E.A., Molodkov A.N., Streletskaya I.D., Vasiliev A.A., Anikina N.Yu., Bondarenko S.A., Derevyanko, L.G., Kupriyanova, N.V., Maksimov, F.E., Polyakova, E.I., Pushina, Z.V., Stepanova, G.V., Oblogov, G.E.: Deposits of the Kazantsevo transgression (MIS-5) in the northern part of the Yenisei catchment. *Russian Geology and Geophysics*, 54 (4), 743-757, 2016b.
- 515 Gutenberg B.: Changes in sea level, postglacial uplift, and mobility of the Earth's intertor // *Geol. Soc. Amer. Bull.*, v. 52, N 5, 251-286, 1941.
- Hughes A.L.C., Gyllencreutz R., Lohne Sh.S., Mangerud J., Svendsen J. I.: The last Eurasian ice sheets – a chronological database and time-slice reconstruction, DATED-1. *Boreas* 45, 1–45, doi: 10.1111 (bor.12142. ISSN 0300-9483), 2016.



- 520 Khrustalev L.N., Emel'yanov N.V., Pustovoi G.P., Yakovlev S.V.: WARM software for calculating the thermal interaction of engineering structures with permafrost. Certificate No. 940281, RosAPO, 1994 (in Russian).
Khutorskoi M.D., Akhmedzyanov V.R., Ermakov A.V., Leonov Yu.G., Podgomykh L.V., Polyak B.G., Sukhikh E.A., Tsybula L.A.: Geothermics of Arctic seas. Transactions, Geological Institute, Issue 605, GEOS, Moscow, 232 pp., 2013 (in Russian).
- 525 Kokin O.V., Tsvetinskiy A.S.: Geocryology of the Ob' Gulf slope contacting fast ice. *Vesti Gazovoi Nauki*, 14, 67-69, 2013.
Kulikov S.N., Rokos S.I.: Detection of permafrost in seismoacoustic time sections from shallow-water areas in the Pechora and Kara seas. *Geofizicheskie Izyskaniya*, 3, 34-42, 2017.
Lamberk K., Chappell J., Sea level change through the Last Glacial cycle. *Science*, 292 (5517), 679-686, 2001.
- 530 Leibman M.O., Kizyakov A.I.: Cryogenic landslides in the Yamal and Yugor Peninsulas. Tipografia Rosselkhozakademiya, Moscow, 206 pp, 2007 (in Russian).
Levitan M.A., Lavrushin Yu.A., Stein R.: Deposition history in the Arctic ocean and Subarctic seas for the past 130 kyr. GEOS, Moscow, 404 pp, 2007 (in Russian).
Levitan M.A.: Quaternary advection of Atlantic waters into the Arctic: a review, in: *Geology and Geoecology of the Eurasian Continental Margins*, Issue 1, GEOS, Moscow, pp. 54-63, 2009 (in Russian).
- 535 Map of Quaternary deposits in the Russian Federation, scale 1:2 500 000, Explanatory note. Minprirody, Rosnedra, VSEGEI, VNII Okeangeologiya, 2010 (in Russian).
Melnikov V.P., Spesivtsev V.I.: Engineering Geological and Geocryological Conditions in the Barents and Kara Seas. Novosibirsk, Nauka, 198 pp, 1995 (in Russian).
- 540 Melnikov V.P., Fedorov K.M., Wolf A.A., Spesivtsev V.I.: Near-bottom ice mounds in the shelf: Possible formation scenario. *Kriosfera Zemli* II (4), 51-57, 1998.
Molodkov A.N., Hutte G.I., Makeev V.M., Baranovskaya O.F., Kosmodamiansky A.V., Ponomareva D.P., Bolshiyarov D.Yu., EPR dating of mollusk shells in Oktyabrskoi Revoliutsii and Koteln'y islands, in: *New Data on Quaternary Geochronology*, Nauka, Moscow, pp. 236-243, 1987 (in Russian).
- 545 Nazarov D.V.: Quaternary Deposits in the Central West Siberian Arctic. Author's Abstract, Candidate Thesis (Geology & Mineralogy). St. Petersburg, 24 pp., 2011 (in Russian).
Neizvestnov Ya.V., Borovik O.V., Kozlov S.A., Kholmyansky M.A.: Subsea permafrost in the Barents, Kara, and Belye seas, in: *Proc. 3rd Conf. of Russian Geocryologists*, Volume 3, Moscow University, Moscow, pp. 184-190, 2005 (in Russian).
- 550 Nikonov A.A.: Holocene and Current Crustal Movements. Nauka, Moscow, 240 pp, 1977 (in Russian).
Parkhomenko S.G.: Sketch Map of Permafrost and Frost Depth in the USSR. Transactions, CNIIGAiK, issue 16, 1937 (in Russian).
Nicol'sky D. J., Romanovskiy V.E., Romanovskii N.N., Kholodov A.L., Shakhova N.T., Semiletov I.P.: Modeling sub-sea permafrost in the East Siberian Arctic Shelf: The Laptev Sea region. *Journal of Geophysical Research*, Issue 117, 2012.
- 555 Art. no. F03028
Pesotsky D.G.: *Qfrost* software for geocryological modeling. Certificate of the State Registration No. 2016614404 of 22 April 2016 (in Russian).
Pogodina I.A.: Spatial distribution and evolution of foraminiferal communities during global climate change. *Vestnik Yuzhnogo Nauchnogo Centra RAN* 5 (2), 64-72, 2009.



- 560 Portnov A., Mienert J., Serov P.: Modeling the evolution of climate-sensitive Arctic subsea permafrost in regions of extensive gas expulsion at the West Yamal shelf. *Journal of Geophysical Research: Biogeosciences* 119 (11), 2082-2094, doi: 10.1002/2014JG002685, 2013.
- Rekant P.V., Vasiliev A.A.: Offshore permafrost in the Kara Sea. *Earth's Cryosphere*, XV (4), 69-72, 2011.
- Rokos S.I., Dlugach A.G., Loktev A.S., Kostin D.A., Kulikov S.N.: Permafrost in the Pechora and Kara shelves: genesis, lithology, and distribution conditions. *Vserossiyskiy Inzhenerno-Analiticheskiy Zhurnal*, 10, 38-41, 2009 (in Russian).
- 565 Rokos S.I., Kostin D.A., Dlugach A.G.: Free gas and permafrost in shallow sediments of the Pechora and Kara shelf areas, in: *Sedimentation Processes and Evolution of Marine Ecosystems in Marine Periglacial Conditions*, Book 1, KNC RAN, Apatity, pp. 40-51, 2001 (in Russian).
- Rokos S.I., Tarasov G.A.: Gas-saturated sediments in estuaries and gulfs in the southern Kara sea. *Bull. Commission on the Quaternary*, 67, 66-75, 2007.
- 570 Romanenko F.A.: Regional evolution features of the Arctic shelf in the Holocene. *Geomorfologiya*, No. 4, 81-92, 2012.
- Romanovsky, N.N., Tumskey, V.E.: Retrospective approach to the assessment of the modern distribution and structure of the shelf cryolithozone of the Eastern Arctic. *Earth's Cryosphere*, Vol. XV, Issue. 1, p. 3-14, 2011.
- Siddall M., Rohling E. J., Almogi-Labin A., Hemleben Ch., Meischner D., Schmelzer I., Smeed D.A.: Sea-level fluctuations during the last glacial cycle. *Nature* 423, 853-858, 2003.
- 575 Siddall M., Chappel, J., Potter E.K.: Eustatic sea level during past interglacials, in: Sirocko, F. et al. (Eds.), *The Climate of Past Interglacials*. Elsevier, Amsterdam, 75 – 92, 2006.
- Siegert M.J., Dowdeswell J.A.: Numerical reconstructions of the Eurasian Ice Sheet and climate during the Late Weichselian. *Quaternary Science Reviews*, 23, 1273-1284, 2004.
- 580 Slichenkov V.I., Samoilovich Yu.G., Nikolaev V.V., Konstantinov V.M.: Structure of Cenozoic sediments in the northern Ob' gulf, Kara Sea; evidence from acoustic data. *Problemy Arktiki i Antarktiki* 82 (2), 106-117, 2009.
- Stein R., Val K., Polyakova E.I., Dittmers K., Postglacial changes in the river runoff and deposition environments in the southern Kara sea, in: *The System of the Laptev Sea and Adjacent Arctic Seas. Current State and Evolution*. Moscow State University, Moscow, 410-426, 2009 (in Russian).
- 585 Streletskaya I.D., Shpolanskaya N.A., Kritsuk L.N., Surkov A.V.: Cenozoic deposits in the Yamal Peninsula and the problem of their origin. *Vestnik Moscow University, Ser. 5. Geografiya* 3, 50-57. Gusev, E.A., Sharin, V.V., Dymov, V.A., Kachurina, N.V., Arslanov, Kh.A., 2012. Shallow sediments in the northern Kara shelf: New data. *Razvedka i Okhrana Nedr*, 8, 87-90, 2009.
- Streletskaya I.D., Gusev E.A., Vasiliev A.A., Rekant P.V., Arslanov Kh.A.: Late Pleistocene-Holocene ground ice in Quaternary deposits on the Kara shelf as a record of paleogeographic conditions. *Bulletin of the Commission on Quaternary* 72, 28-59, 2012.
- 590 Gusev E.A., Sharin V.V., Dymov V.A., Kachurina N.V., Arslanov Kh.A.: Shallow sediments in the northern Kara shelf: New data. *Razvedka i Okhrana Nedr*, 8, 87-90, 2012.
- Streletskaya I.D., Vasiliev A.A., Oblogov G.E., Tokarev I.V.: Reconstruction of paleoclimate of Russian Arctic in Late Pleistocene–Holocene on the basis of isotope study of ice wedges. *Earth Cryosphere*, XIX (2), 98–106, 2015.
- 595 Sulerzhitsky L.D., Tarasov P.E., Andreev A.A., Romanenko F.A.: The Upper Quaternary pollen-based stratigraphy of Sverdrupp Island. *Stratigrafiya. Geologicheskaya Korrelatsiya*, 3 (2), 98-104, 1995.
- Svendsen J., Alexanderson H, Astakhov V., Demidov I., Dowdeswell Ju., Funder S., Gataulin V., Henriksen M., Hjort H., Houmark-Nielsen M., Hubberten H.-W., Ingolfsson O., Jakobsson M., Kjar K, Larsen E., Lokrantz H., Lunkka Ju.P., Lysa A., Mangerud J., Matiouchkov A., Murray A., Moller P., Niessen F., Nikolskaya O., Polyak L., Saarnisto M., Siegert Ch.,
- 600



- Siegert M., Spielhagen R., Stein R.: Late Quaternary ice sheet history of northern Eurasia. *Quaternary Science Reviews*, 23, 1229-1271, 2004.
- The State Geological Map of the Russian Federation Scale 1:1000000 (third generation). Ser. West Siberia, Sheet R-42, Yamal Peninsula, 2015 (in Russian).
- 605 Trofimov V.T. (Ed.): *The Yamal Peninsula (Engineering-Geological Review)*. Moscow State University, Moscow, 278 pp., 1975 (in Russian).
- Trofimov V.T., Badu Yu.B., Kudryashov V.G., Firsov N.G.: *The Yamal Peninsula (Engineering-Geological Review)*. Moscow State University, Moscow, 278 pp., 1975 (in Russian).
- Ushakov S.A., Krass M.S.: *Gravity and Mechanics of the Earth's Interior*. Nedra, Moscow, 157 pp., 1972 (in Russian).
- 610 Vasiliev A.A., Rekant P.V., Oblogov G.E., Korostelev Yu.V.: A new GIS-oriented map of subsea permafrost in the Kara Sea, in: *Proc. Session of Scientific Council on Geocryology*. Russian Academy of Sciences, Volume 1, pp. 291-295, 2018 (in Russian).
- Vasil`chuk Yu.K.: *Oxygen Isotope Composition of Ground Ice: An Experience of Geocryological Reconstructions*. Mosobluprpoligrafizdat, Moscow, Book 1, 420 pp. Book 2, 264 pp., 1992 (in Russian).
- 615 Vasil`chuk Yu.K., Serova A.K., Trofimov V.T.: Deposition environment of Karginian sediments in northern West Siberia. *Bull. Commission for Quaternary* 53, 28-35, 1984.
- Volkov N.G.: *Prediction of Temperature and Major-Ion Chemistry of Pore Water in Saline Permafrost and Cryopegs: Case Study of the Yamal Peninsula*. Author's Abstract, Candidate Thesis (Geology & Mineralogy). Moscow, 26 pp., 2006 (in Russian).
- 620 Yershov E.D.: *Geocryological Map of the USSR, scale 1:2 500 000*. Moscow State University, Moscow, 1991 (in Russian).
- Yershov E.D.: *Geocryology of the USSR. West Siberia*. Nedra, Moscow, 454 pp., 1989 (in Russian).
- Yershov E.D.: *Fundamentals of Geocryology. Part 4. Dynamic Geocryology*. Moscow State University, Moscow, 688 pp., 2001 (in Russian).